

Structural and chemical role of mesenchymal stem cells and resveratrol in regulation of apoptotic -induced genes in Bisphenol-A induced uterine damage in adult female albino rats

Hanan Fouad ^a, Eman Mohamed Faruk ^{b,*}, Wardah Abdullah Alasmari ^c,
Eman Hassan Nadwa ^{d,e}, Usama Fouad Ahmed Ebrahim ^f

^a Medical Biochemistry and Molecular Biology Department, Faculty of Medicine, Cairo University, Cairo, Egypt

^b Department of Histology and Cytology, Faculty of Medicine, Benha University, Benha, Egypt

^c Department of Anatomy Faculty of Medicine, Umm al Qura University, Saudi Arabia

^d Medical Pharmacology Department, Faculty of Medicine, Cairo University, Cairo, Egypt

^e Department of Pharmacology and Therapeutics, Collage of Medicine, Jouf University, Sakaka, Saudi Arabia

^f Anatomy Department, Faculty of Medicine, Benha University, Egypt

ARTICLE INFO

Keywords:

Apoptosis-related genes
TGF- β 1
Oxidative stress markers

ABSTRACT

The probable beneficial effects of mesenchymal stem cells (MSCs) and resveratrol were assessed in an experimental model of Bisphenol-A (BPA)-evident uterine damage in rats. Thirty-five albino rats were involved and equally divided into five groups: Group I: negative control rats received usual diet, Group II: positive control rats received BPA by oral gavage for 15 days, Group III: BPA-treated rats received single oral gavage of resveratrol daily for two weeks, Group IV: BPA-treated rats received a single intravenous dose of MSCs and Group V: BPA-treated rats received combined treatment of resveratrol and MSCs. Oxidative stress markers, apoptosis-related genes, and gonadal hormones were assessed. Histological and immunohistochemical examination of uterine tissue was conducted for TGF- β 1. Caspases-3, 8, and 9 (Casp3, Casp8, Casp9) genes were assessed in uterine tissues by quantitative real-time PCR. Results revealed that BPA induced significant changes in the endometrial tissue, inflammatory cell infiltration, focal blood extravasation, increase in collagen fibers, decrease in PAS staining, and increase in TGF- β 1 immunoreactivity. BPA also induced a significant increase in oxidative stress markers; malondialdehyde (MDA), SOD, CAT, and apoptosis-related genes. BPA induced a significant change in blood levels of gonadal hormones; a significant increase in FSH and a significant decrease in estradiol (E2) and progesterone (P). Treatment with either resveratrol, MSCs, or a combination of them resulted in significant enhancement of histological findings, restoration of gonadal hormones to near-normal levels, and a significant decrease in oxidative stress markers and apoptosis genes. Combined treatment with resveratrol and MSCs demonstrated more significant therapeutic effects as regard to the studied parameters in association with rat groups treated with either MSCs or resveratrol separately.

1. Introduction

Bisphenol A (BPA) is a widely used synthetic chemical in the manufacture of poly-carbonated plastics. Human exposure to BPA always results via leaking and leaching from polycarbonate plastic packages of canned foods and drinks. BPA has been proved to be an estrogen receptor agonist with subsequent feminizing biological effects (Laing et al., 2016). BPA was stated to activate steroidogenic gene transcription, which is responsible for transforming androgenic precursors into

estrogens. Activation of aromatase enzyme by BPA occurs significantly in the gonads of both males and females. In the gonads, BPA exposure exerts significant modulatory influences on genes involved in reproductive function and epigenetic modification signaling (Ziv-Gal and Flaws, 2016). Bisphenol A affect reproductive functions in zebrafish ovary by impaired oxidative/nonoxidative enzymes, apoptotic and inflammatory mediators (Biswas et al., 2020).

BPA, as an endocrine disruptive chemical, was reported to induce short- and long- term effects by modulating the expression of genes

* Corresponding author at: Histology and Cell Biology Department, Faculty of Medicine, Benha University, 44519, Egypt.

E-mail addresses: emkandel@uqu.edu.sa, eman.alsayed@fmed.bu.edu.eg (E.M. Faruk).

<https://doi.org/10.1016/j.tice.2021.101502>

Received 14 December 2020; Received in revised form 23 January 2021; Accepted 24 January 2021

Available online 29 January 2021

0040-8166/© 2021 Published by Elsevier Ltd.

affecting gonadal development. BPA exerts several epigenetic modifications such as production of non-coding RNAs, histone acetylation/ or methylation, and methylation of CpG island promoters (Chianese et al., 2018). Furthermore, BPA exerts negative impacts on histone hyper-acetylation, spermatogenesis, and chromatin fragmentation with subsequent inhibition of embryonic development (González-Rojo et al., 2019). BPA exposure leads to significant activation of caspase 3, which results in augmentation of luteal regression and follicular atresia. Furthermore, estradiol synthesis was significantly decreased via down-regulation of the aromatase synthetic enzyme. BPA selectively down-regulates aromatase cytochrome P450 (P450arom) and the steroidogenic acute regulatory protein (STAR) (Caserta et al., 2014; Peretz et al., 2011).

The use of mesenchymal stem cells (MSCs) exhibits unique therapeutic values because they have great potential to support the regeneration and differentiation of cells and tissues from the three germ layers leading to replacement of tissues destroyed by different injurious stimuli (Liu et al., 2019a,2019b,2019c; Yan et al., 2019). Also, MSCs have been proved to exert significant antiapoptotic effects via downregulation of the caspase-3 mediated apoptotic pathway (Dasari et al., 2007; Liu et al., 2019a). Many studies reported that the in vitro differentiation protocols for the generation of hypothalamic neurons from human pluripotent stem cells (hPSCs) (Wang et al., 2016).

On the other hand, resveratrol is a natural phytoalexin present in many plants. Resveratrol exerts several beneficial effects including anti-atherosclerotic, anti-inflammatory, anti-carcinogenic, anti-obesogenic, antioxidant properties, improving of endothelial function, restoration of NO bioavailability, and the ability to act as Aryl Hydrocarbon Receptors (AHR) antagonist. Furthermore, resveratrol has been reported to prevent BPA-induced vascular toxicity (Hsu et al., 2019a,2019b). Resveratrol has significant protective effects against ovarian and uterine damage induced by methotrexate, irradiation, and other injurious agents (Atli et al., 2017; Amaya et al., 2014). Resveratrol may correct certain outcomes of PCOS patients, through changing the serum levels of sex hormones and expression of *VEGF* & *HIF1* genes (Bahramrezaei et al., 2019).

The present study was conducted to evaluate the potential therapeutic effects of MSCs as well as resveratrol in an experimental model of BPA-induced uterine damage in adult female albino rats.

2. Materials and methods

Thirty-five female adult albino rats (Wistar strain) about six to eight weeks of age (150–250 g BW) were obtained from an inbred colony in the animal house of the Faculty of Medicine, Cairo University. Animals were housed at constant temperature ($22 \pm 2^\circ\text{C}$) and humidity (60 %), with a 12:12 h light: dark cycle and unrestricted access to water. They received a balanced pellet diet (standard RM3 rat chow ad libitum (SDS Ltd, Betchworth, Surrey, UK). All animals were allowed two weeks for acclimatization.

Animals were equally divided into five groups (n = 7/group):

Group I (Control group; negative control). Included normal rats that represent negative control, received the usual diet and bred for 30 days.

Group II (BPA group; pathological control). (BPA was bought from Sigma chemical Company St, Louis, MO, USA)(CAS Number 96210-87-6) then diluted with olive oil to obtain a final concentration of 20 mg/kg body weight (bw) and rats that received daily oral gavage of BPA (20 mg BPA /kg Bwt/day) for 2 weeks at a dosing volume of 0.25 mL/100 g BW.

(Siracusa et al., 2018).

Group III (BPA & Resveratrol group) (Resveratrol was bought from Sigma Chemicals, St, Louis, MO, USA)(CAS Number: 501-36-0): Included rats that received BPA as previously described then received a dose of resveratrol (20 mg/kg Bwt /day) by oral gavage after the last dose of BPA for two weeks. Resveratrol was prepared freshly and

dissolved in DMSO: H₂O (1:4) and the dose adjusted to 0.5 mL/100 gm body weight (Park and Pezzuto, 2015).

Group IV (BPA & MSCs group). Included rats that received BPA regimen and intravenously injected with a single dose of PKH26 fluorescent labeled MSCs (10^6 cells) after the last dose of BPA and bred for two weeks (Abd El Samad et al., 2015).

Group V (BPA, combined MSCs and Resveratrol group). Included rats that received BPA regimen and treated with combined MSCs and resveratrol as described previously. Animals were bred for two weeks after treatment (Faruk et al., 2018).

2.1. MSCs isolation and ex vivo expansion

Seven weeks old albino male rats of Wister strain were sacrificed by cervical dislocation. Bone marrow cells were obtained by flushing the femurs and tibias with sterile PBS. After centrifugation was done, 80 ug/mL gentamicin, 10 % selected fetal bovine serum with alpha-MEM supplemented were added to the cell's suspension. MSCs were plated at a density of 1×10^6 nucleated cells/cm². After 72 h, the media was changed to remove the non-adherent cells. When the foci reached confluence, adherent cells were detached with 0.25 % trypsin, 2.65 mM EDTA, centrifuged and sub-cultured at 7.000 cells/cm². After two sub-cultures, adherent cells were characterized and transplanted (Baghaei et al., 2017).

2.2. Immunophenotyping of MSCs

Immunophenotyping was performed by flow cytometric analysis after immunostaining with monoclonal antibodies against CD73 (FITC-conjugated) from BD Pharmingen, USA, and CD90 (PE-conjugated) (Nery et al., 2013).

2.3. Detection of MSCs homing to target tissues

For detection of homing of MSCs into the tissues of rats, cells were labeled with PKH26 Red Fluorescent Cell Linker Kit (Sigma-Aldrich, Egypt). Labeled cells were injected into the tail vein, and then uterine tissues were examined with a fluorescence microscope to ensure homing (Ghasemzadeh-Hasankolaei et al., 2016).

2.3.1. Histological examination and immunohistochemical staining study

Also, confirmation of estrous cycle regularity was done by detection of the estrous cycles two weeks before the beginning of experiment by examination of vaginal smear. At the scheduled time, all animals were in pro-estrus stage. (Ibrahim et al., 2019).

All animals were sacrificed by cervical dislocation. Blood samples were collected for hormonal assessment and the uterine tissues were isolated and managed for histological examination as they were fixed in 10 % buffered formalin solution for 1–2 days, dehydrated in increasing grades of ethanol, then implanted in paraffin and serial sections (3–5 μm thickness) were cut by a rotary microtome (LEICA RM 2125; UK) then subjected to hematoxylin and eosin staining (H&E) (Bancroft and Layton, 2019b), histochemical by Masson's trichrome (Bancroft and Layton, 2019a) and Periodic Acid Schiff's reaction (PAS) (Layton and Bancroft, 2019).

The Paraffin sections were primed at 5 μm thickness, and immunohistochemical examination for transforming growth factor (TGF)- β type 1 was also done.

Immunohistochemistry staining was performed to detect TGF- β type 1 (a fibrotic marker). The anti-TGF- β antibodies were received from Lab Vision, Neo-markers, Fremont, California, USA (94539) and other chemicals for immunohistochemistry were carried from Sigma-Aldrich, Egypt (SRP1427-6GQ) (Jackson and Blythe, 2013). Uterine cells with cytoplasmic reaction were well thought out as positive. Sections were counterstained with hematoxylin. For the negative control slides, the specific primary antibody was interchanged with PBS. Samples of

human prostatic cancer were available from our pathological department as a positive control for TGF- β . Brown cytoplasmic color was appeared in all positive cells of TGF- β 1.

2.3.2. Morphometric analysis

The mean area percentage of collagen fiber deposition, mean high endometrial thickness, mean area of TGF- β reactivates, and mean area percentage of polysaccharide substances (PAS) in uterine sampling from all rat groups were calculated as five images from four non-overlapping fields of $\times 400$ /slide from each rat group using the Image-Pro Plus program version 6.0 (Media Cybernetics Inc., Bethesda, Maryland, USA) in the histological department of Cairo University, Faculty of Medicine. All recorded data of all groups were statistically estimated by SPSS (SPSS Inc., Chicago, Illinois, USA) software.

2.3.3. Assessment of oxidative stress markers

Measurements of antioxidant enzymes in the uterine tissues: superoxide dismutase (SOD) and catalase (CAT) enzyme activities were determined. For biochemical estimations (0.5 gm each) of tissue, samples were taken ground with liquid nitrogen in a mortar. The ground tissues were then treated with 4.5 mL of the appropriate buffer. The mixtures were homogenized on ice using an Ultra-Turrax homogenizer for 15 min. Homogenates were used for determination of the enzymatic activities. All assays were carried out at room temperature in triplicate (Wu et al., 2018).

Assay of Superoxide dismutase (SOD) and Catalase (CAT): Commercial kits were used to assess SOD and CAT in uterine tissue according to the manufacturer's recommendations (ThermoFisher scientific, Cat No. EIASODC for SOD, and Cat. No. EIACATC for CAT). Results were expressed as micromole per minute per milligram protein ($\mu\text{Mol}/\text{min}/\text{mg}$ protein) (Atalay et al., 2016). Malondialdehyde (MDA) in the tissues was assessed by commercial kits supplied by Abcam (Catalogue No. ab118970) according to the manufacturer's recommendations.

2.3.4. Gonadal hormone assay

Serum levels of estradiol (E2), progesterone (P), FSH, and LH were assessed before and after treatment with different therapeutic protocols. Hormones were assessed by chemiluminescence based immunoassay using Siemens DPC Immulite $\text{\textcircled{R}}$ 1000 (Siemens Medical Solutions Diagnostics, Los Angeles, CA, United States).

2.4. Assessment of apoptosis-related genes by real-time PCR

Gene expression of caspases 3, 8, 9 (*Casp3*, *Casp8*, *Casp9*) were studied in uterine tissue by quantitative real-time PCR (qRT-PCR) using StepOnePlus™ real-time PCR system (Applied Biosystems, USA). Total RNA was extracted from the tissue using RNeasy Mini Kit (Qiagen, USA, Cat No./ID: 74104). The extracted RNA was quantified by spectrophotometry (JENWAY, USA) at 260/280 nm.

2.5. Primer sequence

PCR primers were attained from GenBank RNA sequences cited at the following website: <http://www.ncbi.nlm.nih.gov/tools/primer-blast> for the selection of the ideal primer pair, the considered factors included melting temperature (T_m : 60–65 °C) and applicant length of about 90–200 bp, as shown in Table 1. PCR primers table: The last gene website Link should be (XR_598347.1) with underscore and Not: (XR:598347.1).

2.6. Real-time quantitative PCR using SYBR green

Step One plus real-time PCR system was used in the analysis using software version 3.1 (Applied Biosystems, United States). Optimization of the annealing temperature was conducted for the PCR protocol and for the primer sets. cDNA was prepared for all studied genes,

Table 1

PCR primers.

NM_012922.2 Rattus norvegicus caspase 3 (<i>Casp3</i>), mRNA
Forward primer 3'- GGAGCTTGGAAACGCGAAGAA-5'
Forward primer 3'- ACACAAGCCCATTTGAGGT-5'
NM_022277.1 Rattus norvegicus caspase 8 (<i>Casp8</i>), mRNA
Forward primer 5'- CAGCCTATGCCACCTAGTGATT-3'
Reverse primer 5'- CTGTAACCTGTCCGCGAGTC-3'
NM_031632.1 Rattus norvegicus caspase 9 (<i>Casp9</i>), mRNA
Forward primer 3'- AGCTGGCCAGTGTGAATAC-5'
Reverse primer 3'- GCTCCACCTCAGTCAACTC-5'
XR_598347.1 Glyceraldehyde-3-phosphate dehydrogenase (<i>GAPDH</i>)
Forward primer 5'- GATGCTGGTGTCTGAGTATGTCG -3'
Reverse primer 5'- GTGGTGCAGGATGCATTGCTGA -3'

Real-time quantitative PCR using SYBR Green.

glyceraldehyde 3-phosphate dehydrogenase (*GAPDH*), and for the negative control (non-template). Five microliters of total RNA were used to synthesize cDNA with 20 pmol antisense primers and 0.8 μl Super-script IV Reverse Transcriptase (ThermoFisher, Cat No. 18090010) at 37 °C for 60 min. The relative quantitation of target genes was evaluated using SYBR® Green master mix (Applied Biosystems, CA, United States, Cat No. 4309155). Reaction solution of SYBR Green master mix contains 3 μl of cDNA, 900 nmol/L of each PCR primer pair. Annealing temperature was adjusted at 60°C for all primers. Amplification conditions were conducted according to the manufacturer specifications: 2 min at 50 °C, 10 min at 95 °C, 40 repeated cycles with 15 s denaturation, and 10 min of annealing/extension at 60 °C.

2.7. Calculation of relative quantification (relative expression)

Relative gene expressions of all assessed genes were calculated using the comparative Cycle threshold (Ct) method. The PCR data results show Ct values of the target genes and the house keeping gene (*GAPDH*). A negative control sample was found that no template cDNA was used. Data was calculated using the Applied Biosystems Step One plus software. All values were normalized to *GAPDH* housekeeping gene and expressed as fold changes relative to the background levels found in the control samples.

2.8. Statistical analysis

Continuous variables were presented as the mean \pm SD. Equality of variance was tested by Bartlett's test. A one-way ANOVA or Welch's ANOVA according to equality of variance was used to identify statistical differences between groups. Furthermore, post hoc tests (Tukey test if equal variances are assumed; Tamhane's T2 test if equal variances are not assumed) were performed for multiple comparisons between the experimental groups. The differences were considered significant at $p < 0.05$. All statistical comparisons were two-tailed. All statistical analyses were performed using Graph pad Prism, Version 8.0 Software (Graph Pad Software, San Diego, CA, USA).

3. Results

3.1. MSCs identification and labelling

MSCs were identified in culture medium by their fusiform fibroblast-like cells (Fig. 1A). PKH26 fluorescent labeled MSCs were detected in uterine tissue confirming homing of cells into the target organ (Fig. 1B). Negative control of PKH26 fluorescent stain in non-MSc treated group (Fig. 1C). MSCs were also confirmed by detection of surface markers CD73+ve, CD90+ve, and CD34-ve by flow cytometry analysis ($> 90\%$) (Fig. 1D)

3.1.1. Histological and histochemical results

H&E-stained sections examination of the uterus of group I (control

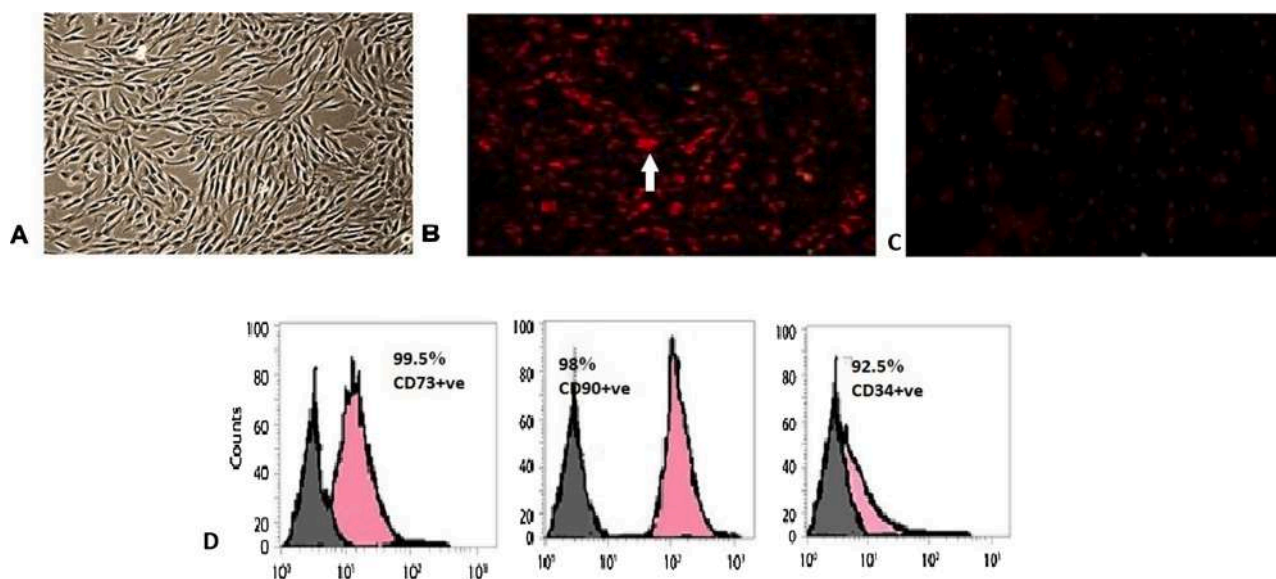


Fig. 1. [A] A photomicrograph of MSCs in culture plate reaching 80 % confluence after 14 days. [B] . A photomicrograph showing homing of PKH26 fluorescent labeled-MSCs into uterine tissue in vitro (arrow). [C] A photomicrograph showing negative control of PKH26 fluorescent stain (non-MSc treated group) in vitro. [D] Flow cytometric characterization analysis showing that MSCs were positive for CD73, CD90 and negative for CD34.

group) displayed normal histological structure of the endometrium, which was lined by surface simple columnar epithelial cells with underlying lamina propria that contained stromal cells, numerous blood vessels and uterine glands. There were well - defined rounded, and elongated uterine glands that were surrounded by epithelioid-like stromal cells (decidual-like cells) and arranged in sheets around the glands, with some spindle-shaped cells (Fig. 2A).

The lining surface epithelium of the endometrium was a secretory epithelium that contained two types of secretory cells: pale cells with pale vesicular nuclei and dark brush border cells with dark irregular nuclei (Fig. 2B). The underlying stroma of the endometrium showed a well-organized stromal cell which were: cells with vesicular nuclei and pale basophilic cytoplasm (decidual like cells), spindle-shaped cells (fibroblast-like cells) (Fig. 2C).

PAS-stained uterine sections of the uterus of the control group showed PAS-positive staining of the basement membranes of the surface columnar cells and the endometrial glands (Fig. 2D). Masson's trichrome-stained sections showed few collagen fibers in the endometrial stroma (Fig. 2E).

H&E-stained uterine sections in **group II (BPA group)** showed multiple changes in the endometrial structure such as a decrease in the epithelial height, the endometrial glands became small and ill-defined with very dense stroma with inflammatory cell infiltration and focal blood extravasation (Fig. 3A). Moreover, the surface epithelium became degenerated and thinned with the presence of empty sub-epithelial spaces and stromal cells revealed a disorganized cellular arrangement with darkly stained nuclei (Fig. 3B and C). PAS-stained uterine sections showed a decrease in PAS-positive staining in the disrupted basement membrane (Fig. 3D). On Masson's trichrome stained sections, there were increases in the content of compacted stromal collagen fibers. (Fig. 3E).

H&E-stained uterine sections in **BPA & Resveratrol group** showed low columnar epithelial endometrial cells with irregular shaped endometrial glands compared to the other treated groups (MSCs and Resveratrol groups) while increased in its epithelium in comparison to BPA group (diseased group) (Fig. 4A). However, the endometrial histology in groups **(BPA & MSCs group)** and **(BPA, combined MSCs and Resveratrol group)** was nearly like the control in which the surface epithelium became columnar with well-developed endometrial glands (Fig. 4D and G).

While PAS-stained sections of the endometrium in groups **BPA & Resveratrol, BPA & MSCs & BPA, and BPA & combined MSCs, and Resveratrol** showed a PAS-positive basement membrane (Fig. 4B, E and H). Examination of Masson's trichrome-stained uterine sections in the same **above groups** revealed a decrease in the collagen content of the endometrial stroma (Fig. 4 C, F, and I) in comparison to the control group. Note that the results of the group **combined MSCs and Resveratrol** is better than in groups **BPA & Resveratrol, BPA & MSCs.**

3.2. Immunohistochemical staining result

Examination of uterine sections from the control group for the immunostaining marker (TGF- β 1) revealed very weak nuclear and cytoplasmic reactivity in the endometrial glandular cells (EGC) and uterine vascular endothelial cells (UVEC) (Fig. 5A), while in **BPA group** revealed a strong nuclear and cytoplasmic reactivity in the endometrial epithelial cells and stromal cells (Fig. 5B and C).

In BPA and Resveratrol, the treated group revealed moderate nuclear and cytoplasmic reactivity in the endometrial epithelial cells and stromal cells (Fig. 5D). However, in groups (BPA & MSCs group) and (BPA & combined MSCs and Resveratrol group) showed mild nuclear and cytoplasmic reactivity in the epithelial and stromal cells (Fig. 5E and F).

3.3. The Morphometric results

Bisphenol-A intoxicated group had significantly lesser endometrial thickness, and area % of polysaccharide substance but significantly greater in area % of TGF- β expression and collagen fibers compared with control group and other treated groups ($P < .05$). Area % of TGF- β 1 expression and polysaccharides substances were not significantly altered in resveratrol, MSCs or their combination ($P > .05$). While the area % of collagen fibers were significantly minimized in MSCs therapy and combined resveratrol and MSCs therapy compared with resveratrol alone ($P < .05$), as shown in Table 2.

3.4. Biochemical results

Bisphenol-A intoxicated group had significantly lower levels of ovarian hormones (E2 and P) but significantly higher levels of FSH hormone compared with control and/ other treatments ($p < 0.05$).

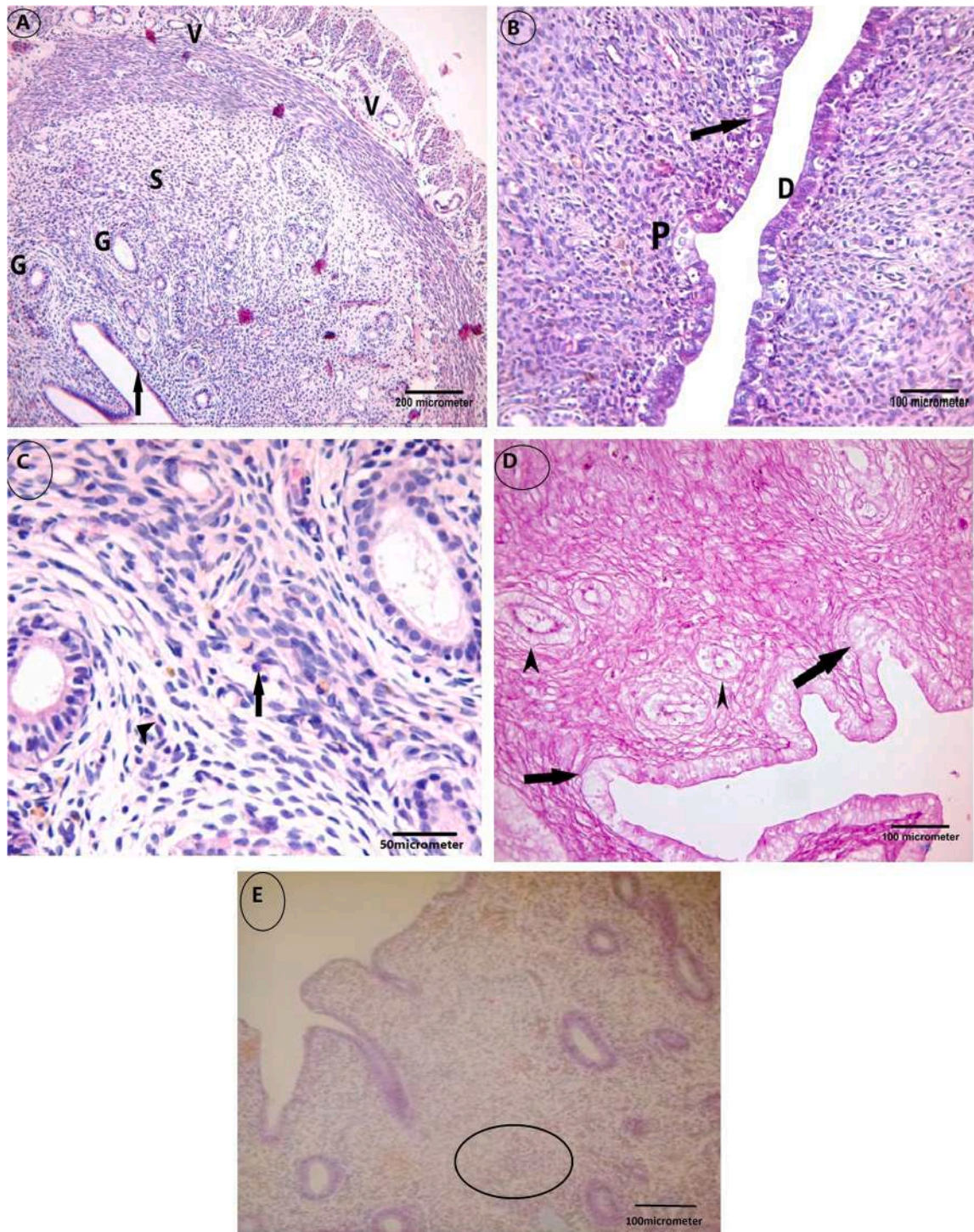


Fig. 2. (A) A photomicrograph of the uterine endometrium showing the lining simple surface columnar epithelial cells (arrow). The highly cellular stroma (S), uterine glands (G) and blood vessels in the myometrium (V). Control group, H&E, $\times 100$, scale bar = 200 μm . (B) surface endometrial epithelium showing the secretory epithelial cells with vacuolated cytoplasm (arrow). Notice that the dark cells (D) and other pale cells (P). Control group, H&E, $\times 200$, scale bar = 100 μm . (C). Higher magnification of stromal cells that are arranged in sheets around the endometrial glands and they are showing cells with vesicular nuclei and pale basophilic cytoplasm (epithelioid-like cells) (arrow) and spindle-shaped cells (fibroblast like cells) (arrowhead). Control group, H&E, $\times 400$, scale bar = 50 μm . (D). The periodic acid–Schiff (PAS) stained uterine section showing positive basement membranes of the surface columnar epithelium (arrows) and around the endometrial glands (arrowhead). Control group, PAS, $\times 200$, scale bar = 100 μm . (E). Masson's trichrome stained endometrial section showing few mildly separated stromal collagen fibers (circle). Control group, Masson's trichrome, $\times 200$, scale bar = 100 μm .

Combined resveratrol and MSCs/ or resveratrol separately produced a significant elevation of estrogen and progesterone levels ($p < 0.05$). Resveratrol and/or MSCs separately or in combination showed a significant decrease in FSH levels ($p > 0.05$). All treatment

regimens did not elicit significant alterations in the levels of LH compared with the control group ($p > .05$), as shown in [Table 3](#).

As regards to oxidative stress markers, the results demonstrated significantly higher levels of MDA enzyme and significantly lower levels

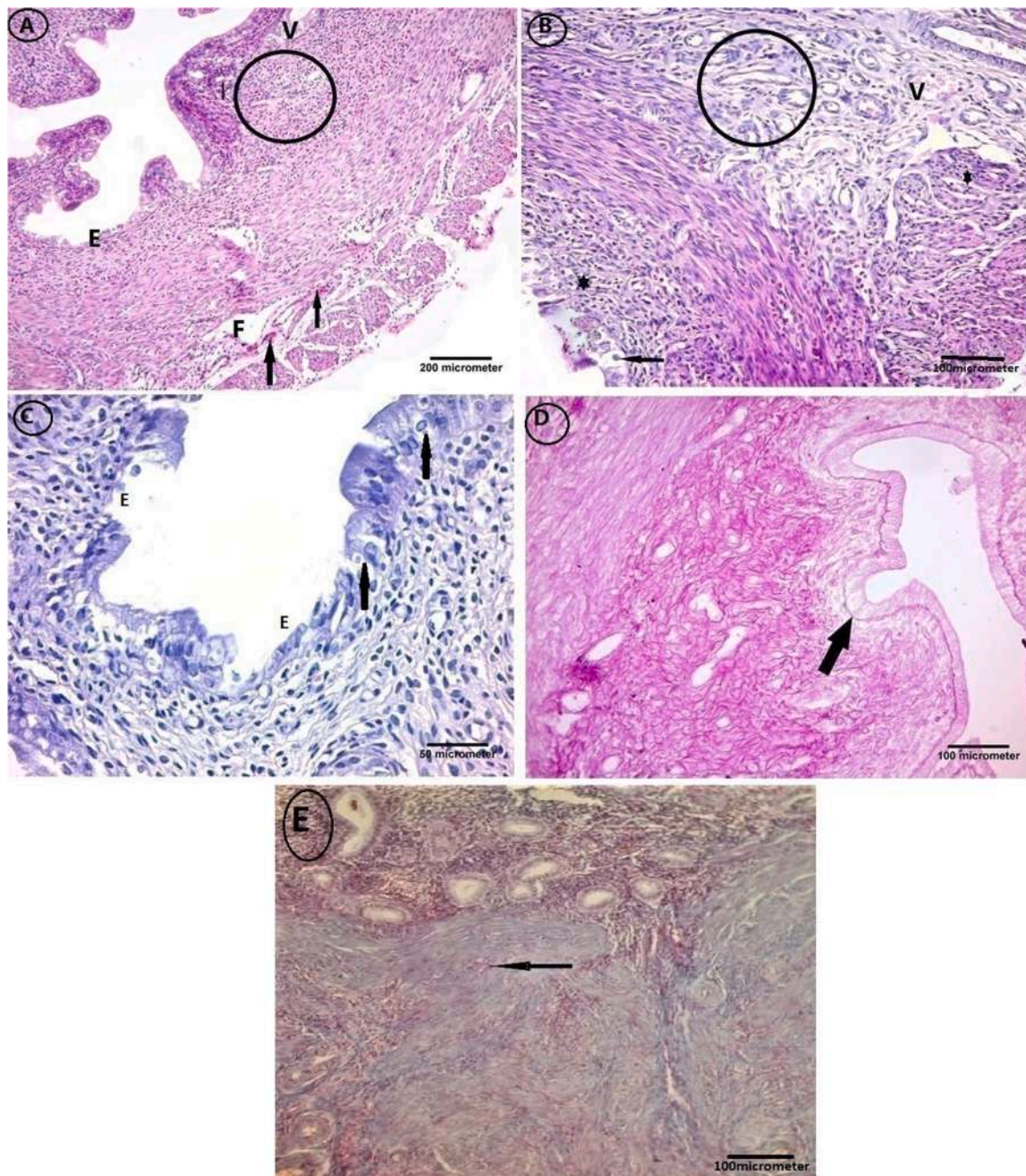


Fig. 3. (A) A photomicrograph of the uterine endometrium showing decrease in the height of the lining epithelium (E). Note the presence of small irregular shaped glands (circle) embedded in very dense cellular stroma with inflammatory cells infiltration (I), blood extravasation (arrows) and separation of muscle fibers (F). Notice congested blood vessels under epithelium (V). Group II, H&E, $\times 100$, scale bar = 200 μm . (B) The uterine endometrium showed degenerated of surface epithelium with vacuolations (arrow), stromal cells showed darkly stained nuclei (star). Note the presence of small irregular shaped glands (circle) Group II, H&E, $\times 200$, scale bar = 100 μm . Notice congested blood vessels under epithelium (V). (C) The endometrial surface epithelium showed degenerated cells (E) with vacuolations (arrows). Group II, H&E, $\times 400$, scale bar = 50 μm . (D) Decrease in periodic acid-Schiff (PAS) positive reaction in the basement membrane of surface epithelium (arrow) and around the endometrial gland (G). Group II, PAS, $\times 200$, scale bar = 100 μm . (E) An apparent increase in the content of the packed stromal collagen fibers, which extend under the lining epithelium (arrow). Group II, Masson's trichrome, $\times 200$, scale bar = 100 μm .

of CAT and SOD enzymes in BPA-treated group compared with control and other treated groups ($p < 0.05$).

Treatment with either MSCs or resveratrol separately showed a significant decrease of MDA and significantly elevated levels of CAT and SOD without normalization of their levels ($p < 0.05$). Combined treatment with MSCs and resveratrol led to normalization of all oxidative stress markers in comparison to the healthy control group (Table 4).

3.4.1. Results of apoptosis-related genes

Results showed that BPA induced a significant increase in *Casp3*, *Casp8*, *Casp9* in uterine tissues in comparison to healthy control animals. Treatment with either MSCs or resveratrol exerted a significant decrease in the three apoptosis genes in comparison to PBA untreated pathological control. Combined treatment with MSCs and resveratrol showed more superior therapeutic effects and significant decrease in *Casp3*, *Casp8*, *Casp9* gene expression with normalization of gene expression levels in comparison to healthy control animals (Fig. 6).

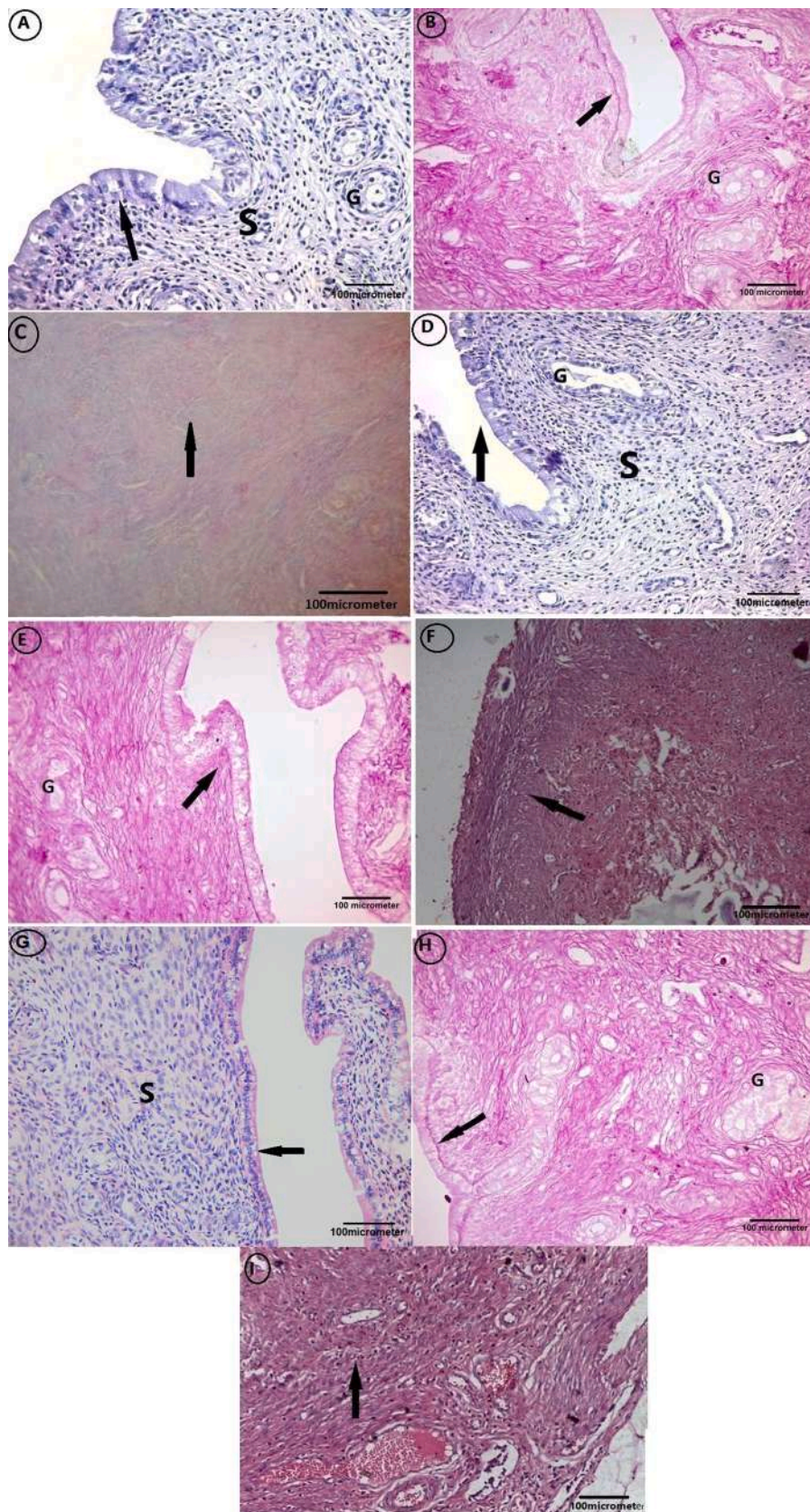


Fig. 4. A photomicrograph of the uterine endometrium (A&D and G) in groups III, IV and V respectively showing an increase in the height of the lining surface epithelium in comparison to diseased group (arrow) with presence of multiple well-developed endometrial glands (G) embedded in cellular stroma (S). Group III, IV and V, H&E, $\times 200$, scale bar = 100 μm). (B&E and H) in groups III, IV and V respectively showing an increase in periodic acid-Schiff (PAS) positive reaction in the basement membrane (arrow) and around the endometrial gland (G). Group III, IV and V, PAS, $\times 200$, scale bar = 100 μm). (C&F and I) in groups III, IV and V respectively showing an apparent decrease in the content of the packed stromal collagen fibers (arrow). Group III, IV and V, Masson's trichrome, $\times 200$, scale bar = 100 μm).

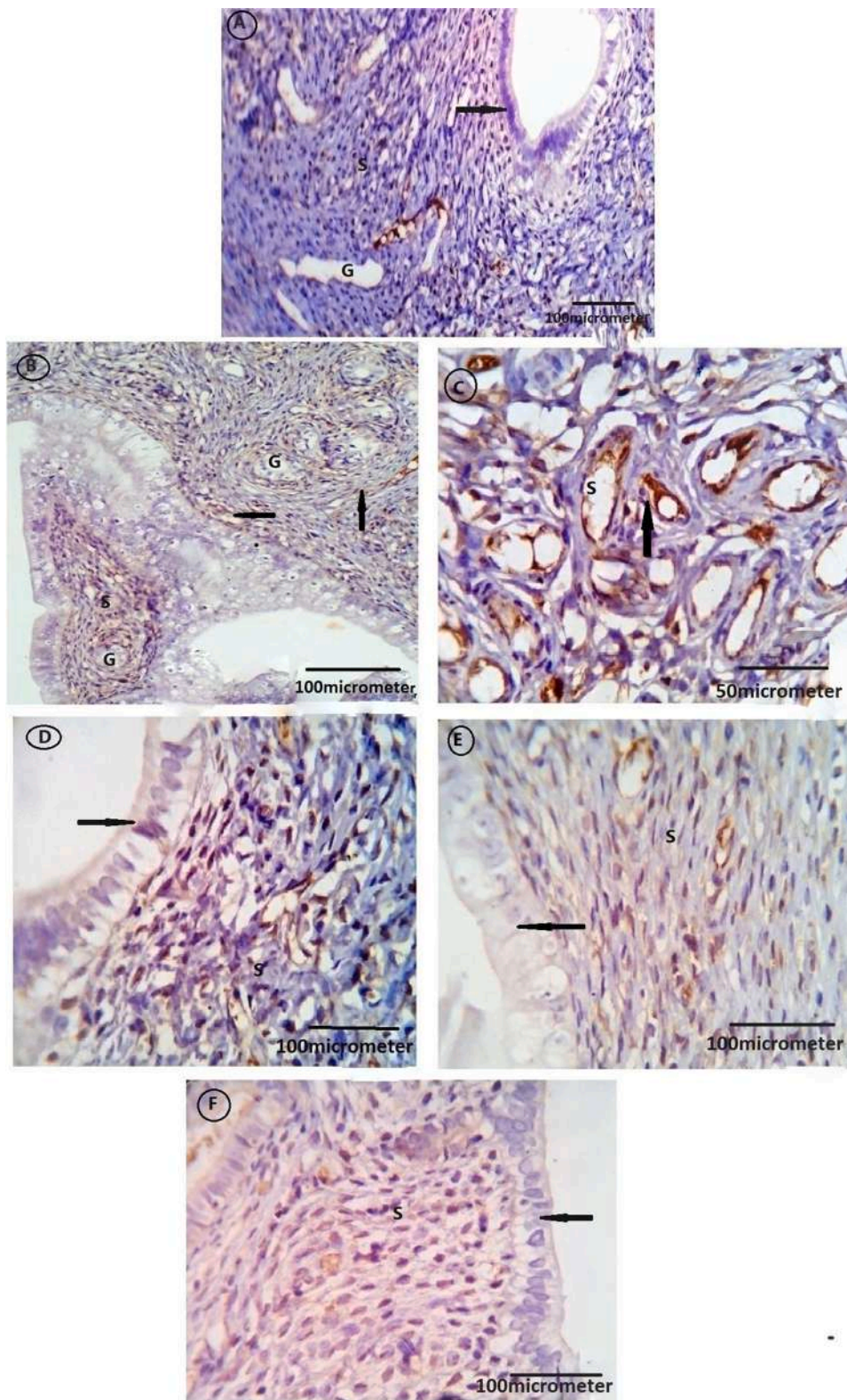


Fig. 5. A) A photomicrograph of rat's uterus immuo-stained by TGF- β of group I, showing very weak nuclear reactivity in most of the endometrial epithelial cells (arrow), gland (G) and stromal cells(S) Scale bars 20,30 μ m. B and C) Rat's uterus immuo-stained by TGF- β in group II, showing strong nuclear reactivity in most of the endometrial epithelial cells (arrow), gland (G) and stromal cells (S). D) Rat's uterus immuo-stained by TGF- β of group III, showing moderate nuclear reactivity in most of the endometrial epithelial cells (arrow), and stromal cells (S). E) and F) Rat's uterus immuo-stained by TGF- β of both group IV and V, showing mild nuclear reactivity in most of the endometrial epithelial cells (arrow) and stromal cells (S). A, B, D, E and F, (Avidine biotin peroxidase stain with Hx counter stain x200, scale bar = 100 μ m).C Avidine biotin peroxidase stain with Hx counter stain x400, scale bar = 50 μ m).

4. Discussion

The damaging effect of Bisphenol A on uterine tissues of rats were assessed in the current study. Histopathological examination of rats exposed to BPA for 15 days showed marked damage in the uterine tissue as evidenced by epithelial degeneration, thinning, and decrease in their height with the presence of empty subepithelial spaces. Endometrial

glands became small, ill-defined with very dense stroma that have inflammatory cell infiltration and focal blood extravasation. Moreover, stromal collagen fibers were markedly increased with a decrease in PAS-positive staining in the disrupted basement membrane. Several studies reported that BPA has long-lasting biological effects on target tissues (Pollock and deCatanzaro, 2014).

The histological findings in this study could be explained by the

Table 2

Effect of mesenchymal stem cells, resveratrol and their combination on height of endometrial thickness, area percent of TGF- β expression, polysaccharides substances and collagen fibers in bisphenol-A induced uterine damage in adult rats.

Parameters	Groups				
	Control	BPA	BPA + Resveratrol	BPA + MSCs	BPA + Resveratrol + MSCs
Height of endometrial thickness (unit)	11.91 \pm 0.8	5.12 \pm 0.07 ^a	9.07 \pm 0.01 ^{ab}	10.24 \pm 0.03 ^{abc}	10.71 \pm 0.025 ^{bcd}
Area % TGF- β expression	1.19 \pm 0.10	3.12 \pm 0.05 ^a	0.97 \pm 0.12 ^{ab}	1.05 \pm 0.12 ^b	1.09 \pm 0.13 ^b
Area % polysaccharides substances	10.15 \pm 1.32	6.12 \pm 0.11 ^a	9.21 \pm 0.82 ^b	9.89 \pm 0.67 ^b	10.01 \pm 1.61 ^b
Area % collagen fibbers	5.95 \pm 0.92	15.72 \pm 1.14 ^a	8.51 \pm 0.73 ^{ab}	6.82 \pm 1.03 ^{bc}	6.31 \pm 1.31 ^{bc}

All values are expressed as mean \pm SD, $n = 7$. ^a significant vs control group, ^b significant vs BPA, ^c significant vs BPA + Resveratrol, ^d significant vs BPA + MSCs ($P < 0.05$) by a one-way ANOVA followed by post hoc Tukey's multiple comparisons test or Welch's one-way ANOVA followed by post hoc Tamhane's T2 multiple comparisons test.

Abbreviations, BPA; Bisphenol-A; MSCs, Mesenchymal stem cells; TGF, Transforming growth factor.

Table 3

Effect of mesenchymal stem cells, resveratrol and their combination on ovarian and pituitary gonadal hormones in bisphenol-A induced uterine damage in adult rats.

Parameters	Groups				
	Control	BPA	BPA + Resveratrol	BPA + MSCs	BPA + Resveratrol + MSCs
Estradiol; E2 (ng/L)	43 \pm 2.13	23.62 \pm 2.24 ^a	33.04 \pm 1.19 ^{ab}	34.6 \pm 0.9 ^{ab}	41.32 \pm 2.6 ^{bcd}
Progesterone; P (ng/mL)	16.42 \pm 1.1	5.14 \pm 0.64 ^a	12.22 \pm 0.85 ^{ab}	13.8 \pm 1.26 ^{ab}	14.19 \pm 1.98 ^{abc}
Serum FSH (IU/L)	10.56 \pm 0.57	17.1 \pm 0.77 ^a	13.18 \pm 1.76 ^b	11.34 \pm 1.61 ^b	10.87 \pm 0.78 ^b
Serum LH (ng/L)	33.46 \pm 0.71	34.18 \pm 3.17	33.4 \pm 2.41	32.26 \pm 3.04	33.15 \pm 1.67

All values are expressed as mean \pm SD, $n = 7$. ^a significant vs control group, ^b significant vs BPA, ^c significant vs BPA + Resveratrol, ^d significant vs BPA + MSCs ($P < 0.05$) by a one-way ANOVA followed by post hoc Tukey's multiple comparisons test or Welch's one-way ANOVA followed by post hoc Tamhane's T2 multiple comparisons test.

Abbreviations, BPA; Bisphenol-A; MSCs, Mesenchymal stem cells; FSH, Follicular stimulating hormone; LH, luteinizing hormone.

study conducted by Pivonello et al., 2020 who stated that BPA can disrupt the hypothalamic pituitary ovarian axis through a damage of gonadotrophin releasing hormone (GnRH) pulsatility, synthesis of ovarian steroid hormones and gonadotrophin signaling. Exposure of uterine epithelial and stromal tissues to BPA may lead to significant morphological and functional changes with subsequent marked decrease in estradiol (E2) and progesterone (P) receptor expression, decline in gene expression of their downstream target genes, enhancement of fibroblast growth factor and MAPK signaling pathways (Li et al.,

Table 4

Effect of mesenchymal stem cells, resveratrol and their combination on oxidative stress markers in uterine tissues in bisphenol-A induced uterine damage in adult rats.

Parameters	Groups				
	Control	BPA	BPA + Resveratrol	BPA + MSCs	BPA + Resveratrol + MSCs
Plasma Malondialdehyde MDA (nMol/L)	9.12 \pm 0.91	22.1 \pm 0.470 ^a	14.9 \pm 0.780 ^{ab}	11.48 \pm 0.711 ^{ab}	10.09 \pm 0.02 ^{bcd}
Uterine MDA (μ Mol/mg protein)	2.14 \pm 0.11	4.6 \pm 0.09 ^a	2.68 \pm 0.21 ^{ab}	3.04 \pm 0.24 ^{ab}	2.2 \pm 0.26 ^{abc}
Uterine CAT (μ Mol/min/mg protein)	6.08 \pm 0.30	4.78 \pm 0.36 ^a	5.72 \pm 0.43 ^b	5.6 \pm 0.4 ^b	6.09 \pm 0.75 ^b
Uterine SOD (μ Mol/min/mg protein)	41.8 \pm 5.11	30.74 \pm 1.74 ^a	40 \pm 1.92 ^{ab}	38.06 \pm 1.88 ^{bc}	42.89 \pm 1.65 ^{bc}

All values are expressed as mean \pm SD, $n = 7$. ^a significant vs control group, ^b significant vs BPA, ^c significant vs BPA + Resveratrol, ^d significant vs BPA + MSCs ($P < 0.05$) by a one-way ANOVA followed by post hoc Tukey's multiple comparisons test or Welch's one-way ANOVA followed by post hoc Tamhane's T2 multiple comparisons test.

Abbreviations, BPA; Bisphenol-A; MSCs, Mesenchymal stem cells; MDA, Plasma Malondialdehyde enzyme; CAT, catalase enzyme.

2016). These facts could explain our findings of the significant increase in collagen fibers in the uterine stroma of BPA exposed rats. Similar findings were reported by Kendziorski and Belcher, 2015. Moreover, BPA-exposure induces mitochondrial dysfunction and apoptosis in the liver and colon of animals (Wang et al., 2019). The authors reported a significant increase in the apoptosis enzymes caspases -3, -8, -9, and -10 after dietary intake of PBA. These findings coincide with our results in which a significant increase in gene expressions of Casp3, Casp8, Casp9 in PBA-exposed untreated rats' group.

As regards to oxidative stress markers, the results of the present study demonstrated significant increase in malondialdehyde (MDA), a significant decrease in SOD and CAT in the uterine tissue of BPA exposed animals. Our findings are in accordance with results reported by Gassman, 2017 who stated that BPA exposure leads to oxidative stress as evidenced by a significant elevations in reactive oxygen species generation (ROS) which initiates numerous cytotoxic, genotoxic and carcinogenic effects on several target tissues and organs. Strong correlations have been previously reported between BPA exposure and elevated levels of lipid peroxidation markers (MDA), and oxidative DNA damage, 8-hydroxydeoxyguanosine (8-OHdG) (Erden et al., 2014; Piao et al., 2019).

Use of resveratrol in the present study exhibited significant protective effects against BPA-induced uterine damage as shown by the significant decrease in oxidative stress markers, apoptosis genes, significant decrease in collagen fibers, significant increase in PAS stained tissues and amelioration of the histological changes induced by BPA. More protective effects against BPA was shown by combined treatment of MSCs and resveratrol as exhibited by restoration of the uterine histology to a near normal picture. Our findings could be explained by a previous study conducted by Hsu et al., 2019a,2019b who stated that resveratrol exerts significant protective effects against the estrogenic effects of BPA as exhibited by the decrease in oxidative stress markers, restoration of nitric oxide bioavailability, and abrogation of Aryl hydrocarbon receptor (AHR) activation; a xenobiotic receptor. Furthermore, resveratrol use has been reported to decrease 8-OHdG; a

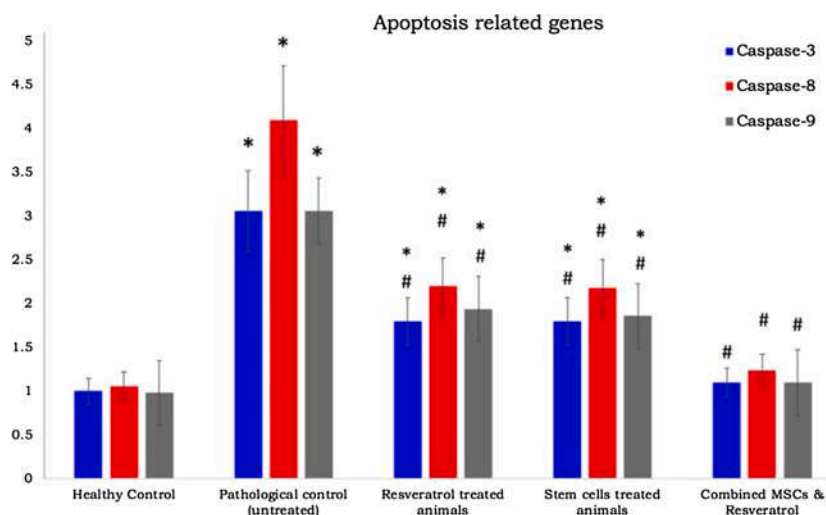


Fig. 6. Apoptosis-related gene expressions (Casp3, Casp8, Casp9) in the studied groups. * significant changes ($p < 0.05$) in comparison to healthy control, # significant changes in comparison to pathological untreated control ($p < 0.05$).

marker of DNA damage induced by oxidative stress (Rameshrad et al., 2018). Resveratrol has also been shown to inhibit apoptosis in several tissues (Senturk et al., 2018; Yingjie et al., 2019).

Moreover, resveratrol was shown to exert significant inhibitory effects on extracellular matrix accumulation in fibrotic diseases such as leiomyoma (Chen et al., 2019). This study supports our findings of the significant decrease in collagen fiber deposition in uterine tissue when using resveratrol. In an experimental model of wound healing, resveratrol use led to a significant increase in VEGF expression and uterine wall thickness during the healing phase (Sayin et al., 2017). These facts support our findings of the significant increase in uterine wall thickness after resveratrol administration to BPA treated rat group.

Also, Resveratrol lead to apoptosis and reduces proliferation of rat ovarian theca cells and decreases androgen levels by arresting Cyp17a1 gene expression (Ortega et al., 2012).

Pang et al., 2015 showed the effect of trans-resveratrol on post-stroke depression via regulation of hypothalamus pituitary adrenal axis as the use of resveratrol in stroke rats showed alterations on gonadotropin expression in the frontal cortex, hippocampus and hypothalamus of those stroke rats indicating the improvement of neuroendocrine system.

As regards to MSCs, results of the present study showed that MSCs either separate, or in combination with resveratrol, exert significant protective effects against BPA-induced endometrial damage. This was shown by the significant increase in endometrial thickness, PAS stained tissue and the significant decrease in collagen fibers and malondialdehyde; an oxidative stress marker. MSCs induced a significant decrease in apoptosis gene expression. MSCs use led also to restoration of sex steroid hormones to near normal levels. Up to our best of knowledge, there are no previous studies conducted on the use of MSCs on BPA-induced uterine damage. However, MSCs have been shown to exert significant protective effects on other uterine disorders.

Gao et al., 2019, stated that bone marrow derived mesenchymal stem cells played important roles in the improvement of reproductive outcomes and in the regeneration of injured endometrium in the experimental models of Asherman' syndrome (AS). The authors noticed significant restoration of proliferation in all layers of rat endometrium. Masson Trichrome staining demonstrated a significant decline in fibrous tissues in the damaged endometrium of MSCs treated rat group. These findings could explain our results of the restoration of near-normal endometrial histology in the rat group treated with MSCs. Moreover, BPA was proved to enhance apoptosis in endometrial tissues at a dose of 25,000 $\mu\text{gBPA}/\text{kg bw}/\text{day}$, which approximates the dose used in the present study (Delclos et al., 2018) MSCs was reported to exert anti-apoptotic effects in female reproductive tissues (He et al., 2018; Yang

et al., 2017).

He et al., 2018, stated the possible therapeutic mechanisms of bone marrow derived MSCs in chemotherapeutics-induced gynecological endocrine disorders. MSCs secrete a myriad of cytokines that are effective for anti-apoptosis, antifibrosis, angiogenesis, anti-inflammation, immunoregulation, and reduction of oxidative stress. Among these cytokines are hepatocyte growth factor (HGF), vascular endothelial growth factor (VEGF), insulin-like growth factor-1 (IGF-1), transforming growth factor (TGF), basic fibroblast growth factor (bFGF), and granulocyte macrophage colony-stimulating factor (GM-CSF) which contribute to inhibition of apoptosis. HGF, bFGF, and adrenomedullin (ADM) are also secreted by MSCs and have significant antifibrotic effects. VEGF, IGF, and monocyte chemo-attractant protein-1 (MCP1) play important roles in angiogenesis. MSCs also protect tissues by inhibition of the inflammatory response and the decrease in oxidative stress. MSCs influence the immune system through several cytokines, such as interleukin (IL)-6 and others (He et al., 2018; Maiborodin et al., 2011).

Moreover, MSCs exert a significant effect on the restoration of sex steroid hormone synthesis after ovarian damage due to different injurious stimuli (Khanmohammadi et al., 2018). Sex steroid hormone play significant effects on endometrial biological functions. All the aforementioned studies support our findings of the significant protective roles of MSCs, either separate or in combination with resveratrol in BPA-induced uterine damage.

In conclusion, the use of either MSCs or resveratrol separately or in combination exerted a significant protective effect against BPA-induced uterine damage via several molecular mechanisms. Restoration of normal gonadal hormone synthesis, decrease in oxidative stress, decrease in apoptosis, antifibrotic effects, and amelioration of histological damage are among the molecular mechanisms exerted by MSCs and resveratrol. Combined treatment of both regimens exhibited superior therapeutic effects than the separate treatment protocol. MSC infusion seemed to restore the BPA effects. However, the mechanism of MSC action is still speculative, and further analysis may be required.

Statement of ethics

Animals were held at the Laboratory Experimental Animal House Unit at Cairo University Cairo, Egypt. After getting the approval of the Ethical Committee for the experimental use of laboratory animals (Approval Number IORG0010305).

Funding sources

Funding for this project was provided by the authors themselves.

Author contributions

Eman Faruk: Writing the paper, searching the data, and doing the histological sections. Wardah Abdullah: Collecting literature search. Hanan Fouad: Writing the paper and literature search. Usama Fouad: preparing the cells and doing the biochemical analysis. Hanan Fouad: doing the gene analysis.

Declaration of Competing Interest

The authors certify that they have no affiliation with or involvement in any organization or entity with any financial or nonfinancial interest in the subject matter or materials discussed in this paper. All the authors read and approved this paper.

References

- Abd El Samad, A.A., Raafat, M.H., Shokry, Y., 2015. Histological study on the role of bone marrow-derived mesenchymal stem cells on the sciatic nerve and the gastrocnemius muscle in a model of sciatic nerve crush injury in albino rats. *EJH* 38, 438–451.
- Amaya, S.C., Savaris, R.F., Filipovic, C.J., Wise, J.D., Hestermann, E., Young, S.L., Lessey, B.A., 2014. Resveratrol and endometrium: a closer look at an active ingredient of red wine using *in vivo* and *in vitro* models. *Reprod. Sci.* 21 (11), 1362–1369. <https://doi.org/10.1177/1933719114525271>.
- Atalay, F., Odabasoglu, F., Halici, M., et al., 2016. N-acetyl cysteine has both gastro-protective and anti-inflammatory effects in experimental rat models: its gastro-protective effect is related to its *in vivo* and *in vitro* antioxidant properties. *J. Cell. Biochem.* 117, 308–319. <https://doi.org/10.1002/jcb.25193>.
- Atli, M., Engin-Ustun, Y., Tokmak, A., Caydere, M., Hucumenoglu, S., Topcuoglu, C., 2019. Dose dependent effect of resveratrol in preventing cisplatin-induced ovarian damage in rats: an experimental study. *Reprod. Biol.* 17 (3), 274–280. <https://doi.org/10.1016/j.repbio.2017.07.001>.
- Baghaei, K., Hashemi, S.M., Tokhanbigli, S., Asadi Rad, A., Assadzadeh-Aghdaci, H., Sharifian, A., Zali, M.R., 2017. Isolation, differentiation, and characterization of mesenchymal stem cells from human bone marrow. *Gastroenterol. Hepatol. Bed Bench* 10 (3), 208–213. PMID: PMC5660271.
- Bahramrezaie, M., Amidi, F., Aleyasin, A., Saremi, A., Aghahoseini, M., Brenjian, S., Khodarahmian, M., Pooladi, A., 2019. Effects of resveratrol on VEGF & HIF1 genes expression in granulosa cells in the angiogenesis pathway and laboratory parameters of polycystic ovary syndrome: a triple-blind randomized clinical trial. *J. Assist. Reprod. Genet.* 36 (August (8)), 1701–1712.
- Bancroft, J.D., Layton, C., 2019a. Connective tissue and other mesenchymal tissues with their stains. In: Suvarna, S.K., Layton, C., Bancroft, J.D. (Eds.), *Bancroft's Theory and Practice of Histological Techniques*, 8th edn. Elsevier, pp. 153–175.
- Bancroft, J.D., Layton, C., 2019b. The hematoxylin and eosin. In: Suvarna, S.K., Layton, C., Bancroft, J.D. (Eds.), *Bancroft's Theory and Practice of Histological Techniques*, 8th edn. Elsevier, Philadelphia, pp. 126–138.
- Biswas, S., Ghosh, S., Samanta, A., Das, S., Mukherjee, U., Maitra, S., 2020. Bisphenol A impairs reproductive fitness in zebrafish ovary: potential involvement of oxidative/nitrosative stress, inflammatory and apoptotic mediators. *Environ. Pollut.* 267 (December), 115692.
- Caserta, D., Di Segni, N., Mallozzi, M., Giovanale, V., Mantovani, A., Marci, R., Moscarini, M., 2014. Bisphenol A and the female reproductive tract: an overview of recent laboratory evidence and epidemiological studies. *Reprod. Biol. Endocrinol.* 12, 37. <https://doi.org/10.1186/1477-7827-12-37>.
- Chen, H.Y., Lin, P.H., Shih, Y.H., Wang, K.L., Hong, Y.H., Shieh, T.M., Huang, T.C., Hsia, S.M., 2019. Natural Antioxidant Resveratrol Suppresses Uterine Fibroid Cell Growth and Extracellular Matrix Formation *In Vitro* and *In Vivo*. *Antioxidants (Basel)* 8 (4). <https://doi.org/10.3390/antiox8040099> pii: E99.
- Chianese, R., Troisi, J., Richards, S., Scafuro, M., Fasano, S., Guida, M., Pierantoni, R., Meccariello, R., 2018. Bisphenol A in reproduction: epigenetic effects. *Curr. Med. Chem.* 25 (6), 748–770. <https://doi.org/10.2174/0929867324666171009121001>.
- Dasari, V.R., Spomar, D.G., Cady, C., Gujrati, M., Rao, J.S., Dinh, D.H., 2007. Mesenchymal stem cells from rat bone marrow downregulate caspase-3-mediated apoptotic pathway after spinal cord injury in rats. *Neurochem. Res.* 32 (12), 2080–2093. <https://doi.org/10.1007/s11064-007-9368-z>.
- Delclos, K.B., Camacho, L., Lewis, S.M., Vanlandingham, M.M., Beland, F.A., Bryant, M. S., Carroll, K.A., Felton, R.P., Gamboa da Costa, G., Howard, P.C., Olson, G.R., Patton, R., Walker, N.J., 2018. NTP Research Report on the CLARITY-BPA Core Study: A Perinatal and Chronic Extended-Dose-Range Study of Bisphenol A in Rats. Division of the National Toxicology Program, National Institute of Environmental Health Sciences, Research Triangle Park, North Carolina, USA. Research Triangle Park (NC): National Toxicology Program; Sep. Report No.: Research Report 9.
- Erden, E.S., Motor, S., Ustun, I., Demirkose, M., Yuksel, R., Okur, R., Oktar, S., Yakar, Y., Sungur, S., Gokce, C., 2014. Investigation of Bisphenol A as an endocrine disruptor, total thiol, malondialdehyde, and C-reactive protein levels in chronic obstructive pulmonary disease. *Eur. Rev. Med. Pharmacol. Sci.* 18 (22), 3477–3483.
- Faruk, E.M., El-desoky, R.E., Al-Shazly, A.M., Taha, N.M., 2018. Do exosomes derived bone marrow mesenchymal stem cells restore ovarian function by promoting stem cell survival on experimentally induced polycystic ovary in adult female albino rats? (Histological and immunohisto-chemical study). *Stem Cell Res. Ther.* 8, 442.
- Gao, L., Huang, Z., Lin, H., Tian, Y., Li, P., Lin, S., 2019. Bone marrow mesenchymal stem cells (BMSCs) restore functional endometrium in the rat model for severe asherman syndrome. *Reprod. Sci.* 26 (3), 436–444. <https://doi.org/10.1177/1933719118799201>.
- Gassman, N.R., 2017. Induction of oxidative stress by bisphenol A and its pleiotropic effects. *Environ. Mol. Mutagen.* 58 (2), 60–71. <https://doi.org/10.1002/em.22072>.
- Ghasemzadeh-Hasankolaei, M., Batavani, R., Eslaminejad, M.B., Sayahpour, F., 2016. Transplantation of autologous bone marrow mesenchymal stem cells into the testes of infertile male rats and new germ cell formation. *Int. J. Stem Cells* 9 (2), 250–263. <https://doi.org/10.15283/ijsc16010>.
- González-Rojo, S., Lombó, M., Fernández-Díez, C., Herráez, M.P., 2019. Male exposure to bisphenol A impairs spermatogenesis and triggers histone hyperacetylation in zebrafish testes. *Environ. Pollut.* 248, 368–379. <https://doi.org/10.1016/j.envpol.2019.01.127>.
- He, Y., Chen, D., Yang, L., Hou, Q., Ma, H., Xu, X., 2018. The therapeutic potential of bone marrow mesenchymal stem cells in premature ovarian failure. *Stem Cell Res. Ther.* 9, 263. <https://doi.org/10.1186/s13287-018-1008-9>.
- Hsu, C.N., Lin, Y.J., Tain, Y.L., 2019a. Maternal exposure to bisphenol A combined with high-fat diet-induced programmed hypertension in adult male rat offspring: effects of resveratrol. *Int. J. Mol. Sci.* 20 (18) <https://doi.org/10.3390/ijms20184382> pii: E4382.
- Hsu, C.N., Lin, Y.J., Tain, Y.L., 2019b. Maternal exposure to bisphenol A combined with high-fat diet-induced programmed hypertension in adult male rat offspring: effects of resveratrol. *Int. J. Mol. Sci.* 20 (18) <https://doi.org/10.3390/ijms20184382> pii: E4382.
- Ibrahim, I.H., Aboregela, A.M., Gouda, R.H., Eid, K.A., 2019. Chronic valproate treatment influences folliculogenesis and reproductive hormones with possible ameliorating role for folic acid in adult albino rats. *Acta Histochem.* 121 (October (7)), 776–783.
- Jackson, P., Blythe, D., 2013. Immunohistochemical techniques. In: Suvarna, S.K., Layton, C., Bancroft, J.D. (Eds.), *Theory and Practice of Histological Techniques*, 7th ed. Churchill Livingstone Elsevier, Philadelphia, PA, pp. 381–426.
- Kendzioriski, J.A., Belcher, S.M., 2015. Strain-specific induction of endometrial periglandular fibrosis in mice exposed during adulthood to the endocrine disrupting chemical bisphenol A. *Reprod. Toxicol.* 58, 119–130. <https://doi.org/10.1016/j.reprotox.2015.08.001>.
- Khanmohammadi, N., Sameni, H.R., Mohammadi, M., Pakdel, A., Mirmohammadkhani, M., Parsaie, H., Zarbakhsh, S., 2018. Effect of transplantation of bone marrow stromal cell- conditioned medium on ovarian function, morphology and cell death in cyclophosphamide-treated rats. *Cell J.* 20 (1), 10–18. <https://doi.org/10.22074/cellj.2018.4919>.
- Laing, L.V., Viana, J., Dempster, E.L., Trznadel, M., Trunkfield, L.A., Uren Webster, T.M., van Aarle, R., Paull, G.C., Wilson, R.J., Mill, J., Santos, E.M., 2016. Bisphenol A causes reproductive toxicity, decreases dnmt1 transcription, and reduces global DNA methylation in breeding zebrafish (*Danio rerio*). *Epigenetics* 11 (7), 526–538. <https://doi.org/10.1080/15592294.2016.1182272>.
- Layton, C., Bancroft, J.D., 2019. Carbohydrates. In: Suvarna, S.K., Layton, C., Bancroft, J. D. (Eds.), *Bancroft's Theory and Practice of Histological Techniques*, 8th edn. Elsevier, Philadelphia, pp. 176–197. 2019.
- Li, Q., Davila, J., Kannan, A., Flaws, J.A., Bagchi, M.K., Bagchi, I.C., 2016. Chronic exposure to Bisphenol A affects uterine function during early pregnancy in mice. *Endocrinology* 157 (5), 1764–1774. <https://doi.org/10.1210/en.2015-2031>.
- Liu, H., Sun, X., Gong, X., Wang, G., 2019a. Human umbilical cord mesenchymal stem cells derived exosomes exert antiapoptosis effect via activating PI3K/Akt/mTOR pathway on H9C2 cells. *J. Cell. Biochem.* 120 (9), 14455–14464. <https://doi.org/10.1002/jcb.28705>.
- Liu, R., Zhang, X., Fan, Z., Wang, Y., Yao, G., Wan, X., Liu, Z., Yang, B., Yu, L., 2019b. Human amniotic mesenchymal stem cells improve the follicular microenvironment to recover ovarian function in premature ovarian failure mice. *Stem Cell Res. Ther.* 10 (1), 299. <https://doi.org/10.1186/s13287-019-1315-9>.
- Liu, Yingjie, Wu, Yiru, Diao, Zongli, Guo, Weikang, Liu, Wenhui, 2019c. Resveratrol inhibits parathyroid hormone-induced apoptosis in human aortic smooth muscle cells by upregulating sirtuin 1. *Ren. Fail.* 41 (1), 401–407. <https://doi.org/10.1080/0886022X.2019.1605296>.
- Maiborodin, I.V., Yakimova, N.V., Matveyeva, V.A., Pekarev, O.G., Maiborodina, E.I., Pekareva, E.O., 2011. Angiogenesis in rat uterine cicatrix after injection of autologous bone marrow mesenchymal stem cells. *Bull. Exp. Biol. Med.* 150 (6), 756–761. <https://doi.org/10.1007/s10517-011-1242-y>.
- Nery, A.A., Nascimento, I.C., Glaser, T., Bassaneze, V., Krieger, J.E., Ulrich, H., 2013. Human mesenchymal stem cells: from immunophenotyping by flow cytometry to clinical applications. *Cytometry A.* 83 (1), 48–61. <https://doi.org/10.1002/cyto.a.22205>.
- Ortega, I., Villanueva, J.A., Wong, D.H., Cress, A.B., Sokalska, A., Stanley, S.D., Duleba, A.J., 2012. Resveratrol reduces steroidogenesis in rat ovarian theca-interstitial cells: the role of inhibition of Akt/PKB signaling pathway. *Endocrinology* 153 (August (8)), 4019–4029.
- Pang, C., Cao, L., Wu, F., Wang, L., Wang, G., Yu, Y., Zhang, M., Chen, L., Wang, W., Lv, W., Chen, L., 2015. The effect of trans-resveratrol on post-stroke depression via regulation of hypothalamus-pituitary-adrenal axis. *Neuropharmacology* 97 (October), 447–456.

- Park, E.J., Pezzuto, J.M., 2015. The pharmacology of resveratrol in animals and humans. *Biochimica et Biophysica Acta (BBA)-Mol. Basis Dis.* 1852 (June (6)), 1071–1113.
- Peretz, J., Gupta, R.K., Singh, J., Hernández-Ochoa, I., Flaws, J.A., 2011. Bisphenol A impairs follicle growth, inhibits steroidogenesis, and downregulates rate-limiting enzymes in the estradiol biosynthesis pathway. *Toxicol. Sci.* 119 (1), 209–217. <https://doi.org/10.1093/toxsci/kfq319>.
- Piao, X., Liu, Z., Li, Y., Yao, D., Sun, L., Wang, B., Ma, Y., Wang, L., Zhang, Y., 2019. Investigation of the effect for bisphenol A on oxidative stress in human hepatocytes and its interaction with catalase. *Spectrochim. Acta A Mol. Biomol. Spectrosc.* 221, 117149 <https://doi.org/10.1016/j.saa.2019.117149>.
- Pivonello, C., Muscogiuri, G., Nardone, A., Garifalos, F., Provisiero, D.P., Verde, N., de Angelis, C., Conforti, A., Piscopo, M., Auriemma, R.S., Colao, A., Pivonello, R., 2020. Bisphenol A: an emerging threat to female fertility. *Reprod. Biol. Endocrinol.* 18 (1), 22. <https://doi.org/10.1186/s12958-019-0558-8>.
- Pollock, T., deCatanzaro, D., 2014. Presence and bioavailability of bisphenol A in the uterus of rats and mice following single and repeated dietary administration at low doses. *Reprod. Toxicol.* 49, 145–154. <https://doi.org/10.1016/j.reprotox.2014.08.005>.
- Rameshrad, M., Imenshahidi, M., Razavi, B.M., Iranshahi, M., Hosseinzadeh, H., 2018. Bisphenol A vascular toxicity: protective effect of *Vitis vinifera* (grape) seed extract and resveratrol. *Phytother. Res.* 32 (12), 2396–2407. <https://doi.org/10.1002/ptr.6175>.
- Sayin, O., Micili, S.C., Goker, A., Kamaci, G., Ergur, B.U., Yilmaz, O., Guner Akdogan, G., 2017. The role of resveratrol on full - Thickness uterine wound healing in rats. *Taiwan J. Obstet. Gynecol.* 56 (5), 657–663.
- Senturk, S., Yaman, M.E., Aydin, H.E., Guney, G., Bozkurt, I., Paksoy, K., Abdioglu, A.A., 2018. Effects of resveratrol on inflammation and apoptosis after experimental spinal cord injury. *Turk. Neurosurg.* 28 (6), 889–896. <https://doi.org/10.5137/1019-5149.JTN.21829-17.3>.
- Siracusa, J.S., Yin, L., Measel, E., Liang, S., Yu, X., 2018. Effects of bisphenol A and its analogs on reproductive health: a mini review. *Reprod. Toxicol.* 79 (August), 96–123.
- Wang, L., Egli, D., Leibel, R.L., 2016. Efficient generation of hypothalamic neurons from human pluripotent stem cells. *Curr. Protoc. Hum. Genet.* 90 (July(1)), 21–25.
- Wang, K., Zhao, Z., Ji, W., 2019. Bisphenol A induces apoptosis, oxidative stress and inflammatory response in colon and liver of mice in a mitochondria-dependent manner. *Biomed. Pharmacother.* 117, 109182 <https://doi.org/10.1016/j.biopha.2019.109182>.
- Wu, X., Huang, Q., Xu, N., et al., 2018. Antioxidative and anti-inflammatory effects of water extract of *Acrostichum aureum* Linn. Against ethanol-induced gastric ulcer in rats. *Evid. Based Complement. Altern. Med.* 2018, 3585394 <https://doi.org/10.1155/2018/3585394>.
- Yan, Z., Guo, F., Yuan, Q., Shao, Y., Zhang, Y., Wang, H., Hao, S., Du, X., 2019. Endometrial mesenchymal stem cells isolated from menstrual blood repaired epirubicin-induced damage to human ovarian granulosa cells by inhibiting the expression of Gadd45b in cell cycle pathway. *Stem Cell Res. Ther.* 10 (1), 4. <https://doi.org/10.1186/s13287-018-1101-0>.
- Yang, H., Wu, S., Feng, R., Huang, J., Liu, L., Liu, F., Chen, Y., 2017. Vitamin C plus hydrogel facilitates bone marrow stromal cell-mediated endometrium regeneration in rats. *Stem Cell Res. Ther.* 8 (1), 267.
- Ziv-Gal, A., Flaws, J.A., 2016. Evidence for bisphenol A-induced female infertility - Review (2007–2016). *Fertil. Steril.* 106 (4), 827–856. <https://doi.org/10.1016/j.fertnstert.2016.06.027> (15).